

Intrinsic magnetism of a series of Co substituted ZnO single crystals

This article has been downloaded from IOPscience. Please scroll down to see the full text article.

2008 J. Phys.: Condens. Matter 20 035206

(<http://iopscience.iop.org/0953-8984/20/3/035206>)

View [the table of contents for this issue](#), or go to the [journal homepage](#) for more

Download details:

IP Address: 129.252.86.83

The article was downloaded on 29/05/2010 at 07:26

Please note that [terms and conditions apply](#).

Intrinsic magnetism of a series of Co substituted ZnO single crystals

Peiwen Lv¹, Feng Huang^{1,4}, Wangsheng Chu², Zhang Lin¹,
Dagui Chen¹, Wei Li¹, Dongliang Chen² and Ziyu Wu^{2,3}

¹ Laboratory of Materials Chemistry and Physics, Fujian Institute of Research on the Structure of Matter, National Engineering Research Center for Optoelectronic Crystalline Materials, Chinese Academy of Sciences, Fuzhou, Fujian 350002, People's Republic of China

² Beijing Synchrotron Radiation Facility, Institute of High Energy Physics, Chinese Academy of Sciences, 100049 Beijing, People's Republic of China

³ National Center for Nanoscience and Technology, People's Republic of China

E-mail: fhuang@fjirsm.ac.cn

Received 13 September 2007, in final form 21 November 2007

Published 17 December 2007

Online at stacks.iop.org/JPhysCM/20/035206

Abstract

Magnetic properties of a series of well-substituted $\text{Zn}_{1-x}\text{Co}_x\text{O}$ ($x = 0.018, 0.036$ and 0.05) single crystals were studied. A typical paramagnetic anisotropy property, which strengthens when x decreases, was found. A magnetization step was observed at 2 K when the magnetic field is parallel to the c axis, indicating that paramagnetic anisotropy is the origin of the strong crystal field effect on Co^{2+} ions in ZnO lattices. The Co^{2+} single-ion anisotropy parameter $2D$ is obtained as 7.5 K. The effective moment of Co^{2+} takes the values $2.7 \mu_B, 1.82 \mu_B, 1.49 \mu_B$ when $x = 0.018, 0.036$ and 0.05 , revealing that more antiferromagnetic coupling between Co^{2+} ions arises in the perfect crystal when x increases.

1. Introduction

Diluted magnetic semiconductors (DMSs) have attracted attention for their potential application in spintronic semiconductor devices [1–3]. Wide band gap semiconductors such as transition metal doped ZnO are predicted to be the most promising candidates for achieving high Curie temperatures [4–7]. Accordingly, numerous groups have reported works related to the magnetic property of Co or Mn doped ZnO thin films and polycrystalline [8–12]. Owing to the lack of reliable identifications and good characterization of the doping situation, contradictory results were reported.

It is believed that high quality single crystals are ideal samples that may provide basic scientific data for understanding the intrinsic magnetic character of transition metal doped ZnO and related DMS phenomena. Previously we have reported that $\text{Zn}_{0.95}\text{Co}_{0.05}\text{O}$ single crystal grown via a hydrothermal method shows typical paramagnetic behavior and a paramagnetic anisotropy property [13]. As pointed out, the anisotropic peculiarities of the magnetization process can be viewed as a signature of intrinsic ferromagnetism in $\text{Zn}_{1-x}\text{Co}_x\text{O}$ materials [14]. Until now, this specific behavior

⁴ Author to whom any correspondence should be addressed.

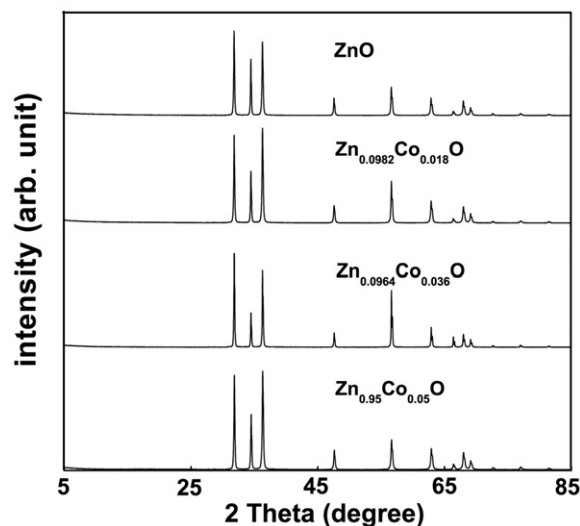


Figure 1. XRD pattern for ZnO and the series of $\text{Zn}_{1-x}\text{Co}_x\text{O}$ single crystals.

has only been confirmed experimentally for the high quality and well characterized $\text{Zn}_{0.95}\text{Co}_{0.05}\text{O}$ single crystal [13]. In

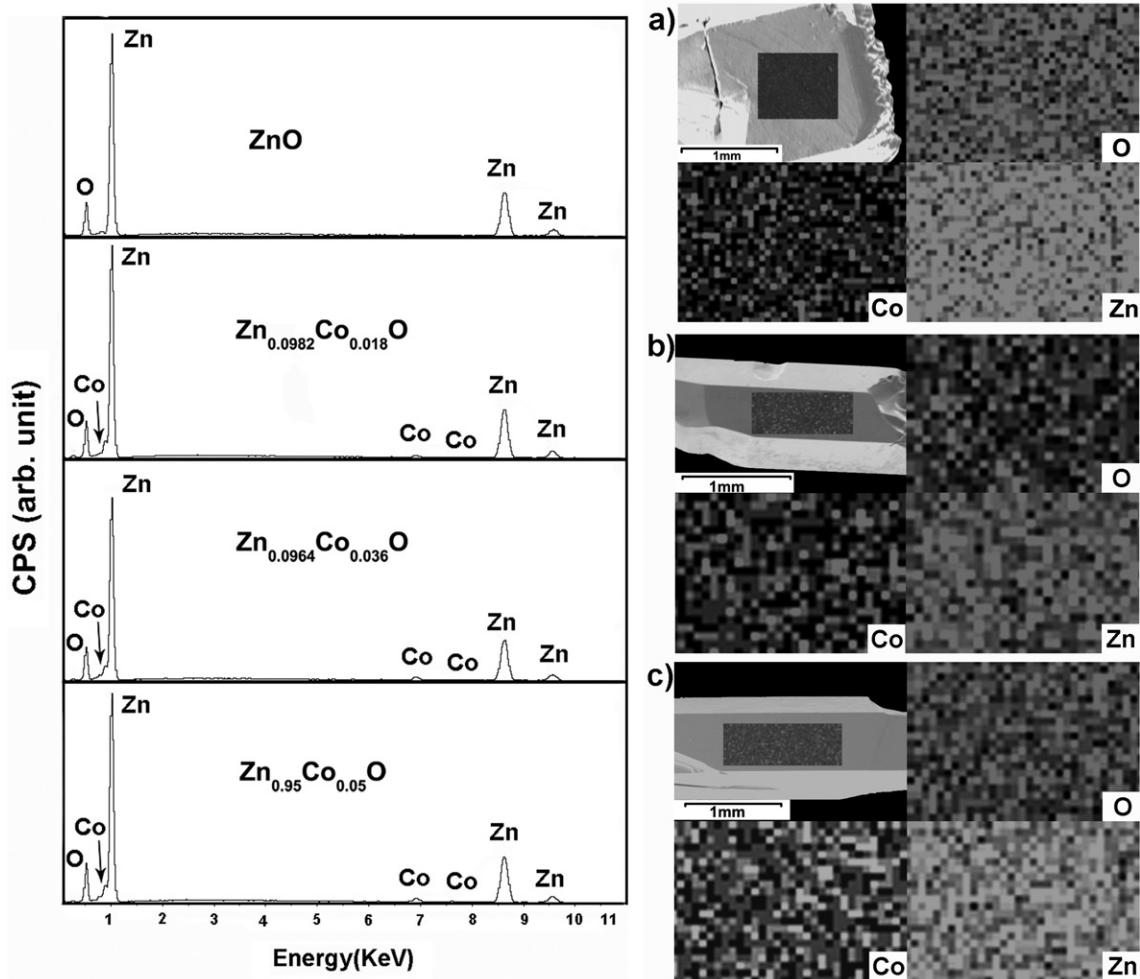


Figure 2. Left: EDX spectra of as-grown single crystals. Right: SEM image of $Zn_{1-x}Co_xO$ single crystals and the AES elemental homogeneity mapping for Co, Zn and O elements on the selected surface area for (a) $Zn_{0.982}Co_{0.018}O$, (b) $Zn_{0.964}Co_{0.036}O$, (c) $Zn_{0.95}Co_{0.05}O$ single crystals. The gray scale is proportional to the surface concentration of the element. It gives a good image of the uniform distribution of Co in the crystal.

this work, a series of high quality $Zn_{1-x}Co_xO$ single crystals were synthesized, for investigating the relationship of doping level, the transition of the magnetic anisotropy property and the intrinsic magnetism of $Zn_{1-x}Co_xO$ materials systematically.

2. Experimental details

The series of $Zn_{1-x}Co_xO$ single crystals were grown by a hydrothermal method. Stainless steel autoclaves with an internal volume of 35 ml were used. A suitable quantity of sintered ZnO, a certain ratio of $CoCl_2$ and a special mineralizer were transferred into the autoclave. After that, the autoclave was put into a furnace with the temperature set at $320^\circ C$ for growing crystals. The crystals were dark green in color and in prism form with a typical size about $1\text{ mm} \times 3\text{ mm}$. The phase compositions and fine lattice changes of the crystals were characterized using Philip's PANalytical X'Pert Pro x-ray diffraction (XRD) and Rietveld refinement. The distribution and concentration of Co in ZnO single crystals were measured with a JSM-6700F scanning electron microscope (SEM)

equipped with an Oxford-INCA energy dispersive x-ray (EDX) spectroscopy. Element components of the crystals were detected by using a Jobin-Yvon Ultima2 inductively coupled plasma (ICP) atomic emission spectrometer (AES) method. Absorbance optical spectra of the crystals were collected using a Perkin-Elmer Lambda-900 ultraviolet-visible (UV) spectrometer at room temperature. For confirming the substitution of Zn^{2+} with Co^{2+} in the crystal lattice, the Co and Zn K-edge extended x-ray absorption fine structure (EXAFS) and x-ray absorption near-edge structure (XANES) spectra were obtained at the XAFS station in the National Synchrotron Radiation Laboratory (NSRL, Hefei) at room temperature. The magnetic properties of the crystals were investigated using the Quantum Design PPMS60000 magnetometer. Carrier concentration and electrical resistivity were measured by the Van Der Pauw method.

3. Results and discussion

The doping levels x for $Zn_{1-x}Co_xO$ single crystals were detected as 0.018, 0.036 and 0.05 (the corresponding Co^{2+}

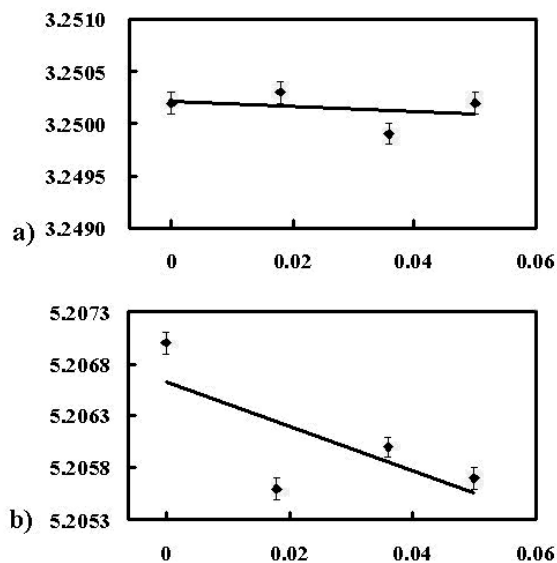


Figure 3. Evolution of cell parameters of $\text{Zn}_{1-x}\text{Co}_x\text{O}$ crystals.

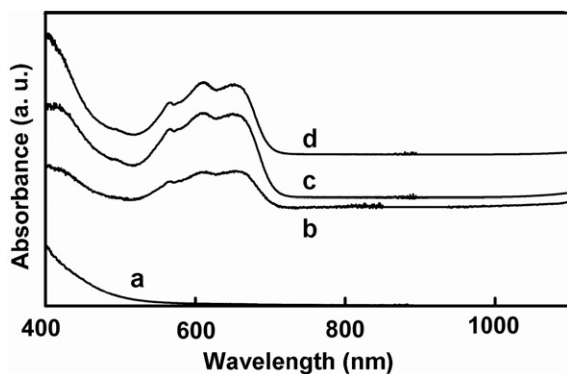


Figure 4. Room temperature optical transmission spectra for (a) ZnO , (b) $\text{Zn}_{0.982}\text{Co}_{0.018}\text{O}$, (c) $\text{Zn}_{0.964}\text{Co}_{0.036}\text{O}$, (d) $\text{Zn}_{0.95}\text{Co}_{0.05}\text{O}$ single crystals. The absorption peaks at around 650, 610, 565 nm can be assigned to ${}^4\text{A}_2(\text{F}) \rightarrow {}^2\text{E}(\text{G})$, ${}^4\text{A}_2(\text{F}) \rightarrow {}^4\text{T}_1(\text{P})$ and ${}^4\text{A}_2(\text{F}) \rightarrow {}^2\text{A}_1(\text{G})$ for Co^{2+} , attributable to the crystal field transitions in the high spin state of Co^{2+} in tetrahedral coordination.

percentages in the starting solution ($\text{Co}:(\text{Co} + \text{Zn})$ were 0.03, 0.05 and 0.10 respectively) by ICP elemental analysis, and further confirmed by SEM-EDX analysis. XRD patterns of the crystals show standard ZnO wurtzite peaks; no other impurity phases were found (figure 1). The uniform distribution of Co in the series of crystals was confirmed by AES mapping (figure 2).

Rietveld analysis shows that there were only slight changes in cell parameters upon doping (figure 3), indicating that Co^{2+} ions have substituted for Zn^{2+} ions and incorporated into the ZnO lattice with tetrahedral coordination [12]. UV spectra of the series of crystals also show typical peaks of ${}^4\text{A}_2(\text{F}) \rightarrow {}^2\text{E}(\text{G})$, ${}^4\text{A}_2(\text{F}) \rightarrow {}^4\text{T}_1(\text{P})$ and ${}^4\text{A}_2(\text{F}) \rightarrow {}^2\text{A}_1(\text{G})$ for Co^{2+} , attributable to the crystal field transitions of the high spin state of Co^{2+} in tetrahedral coordination (figure 4) [15].

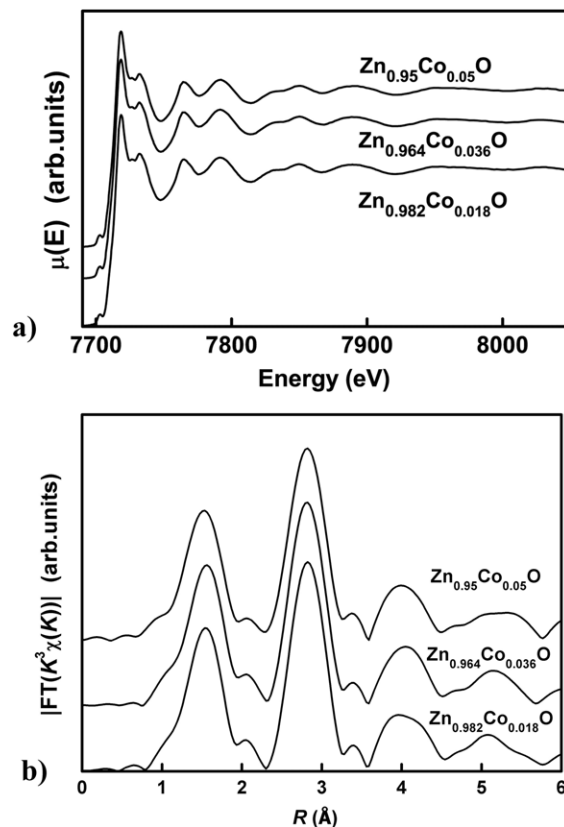


Figure 5. (a) The Co K-edge XANES spectra and (b) Fourier transforms of the k^3 -weighted EXAFS oscillations for the series of $\text{Zn}_{1-x}\text{Co}_x\text{O}$ single crystals.

In order to exclude the possibility of existence of other Co species in the $\text{Zn}_{1-x}\text{Co}_x\text{O}$ single crystals, and further confirm the substitution of Zn^{2+} ion sites with Co^{2+} ions, Co K-edge XANES spectra of the series of crystals were collected. As shown in figure 5(a), the Co K-edge XANES spectra of $\text{Zn}_{1-x}\text{Co}_x\text{O}$ ($x = 0.018, 0.036$ and 0.05) are almost the same. Previously we have identified that Co^{2+} ions have substituted for Zn^{2+} ions and incorporated into the ZnO lattice in $\text{Zn}_{0.95}\text{Co}_{0.05}\text{O}$ single crystal [13]. The similarity of the shoulder, main peak and features at 10–90 eV of the XANES spectra for the series of $\text{Zn}_{1-x}\text{Co}_x\text{O}$ single-crystal samples have excluded the possibility of Co forming the Co clusters and any other cobalt oxides in the samples [13]. In addition, the Fourier transforms of the k^3 -weighted EXAFS oscillations for the series of $\text{Zn}_{1-x}\text{Co}_x\text{O}$ crystals are almost the same (figure 5(b)). We have mentioned previously the similarity of the Co K-edge features of $\text{Zn}_{1-x}\text{Co}_x\text{O}$ crystals with Zn K-edge features of ZnO , indicating that the chemical environment of Co in the series of doped crystals is the same as that of Zn in ZnO [13]. Therefore both XANES and EXAFS results revealed that we have obtained a series of $\text{Zn}_{1-x}\text{Co}_x\text{O}$ single crystals with ideal substitution of Co in the lattice.

Figure 6 shows the magnetization curves of the crystals. For each sample, the temperature dependence of the inverse magnetic susceptibility ($1/\chi$) displays a typical Curie–Weiss behavior ($\chi = C/(T - \Theta)$; C is the Curie constant) in directions parallel and perpendicular to c axis. For both

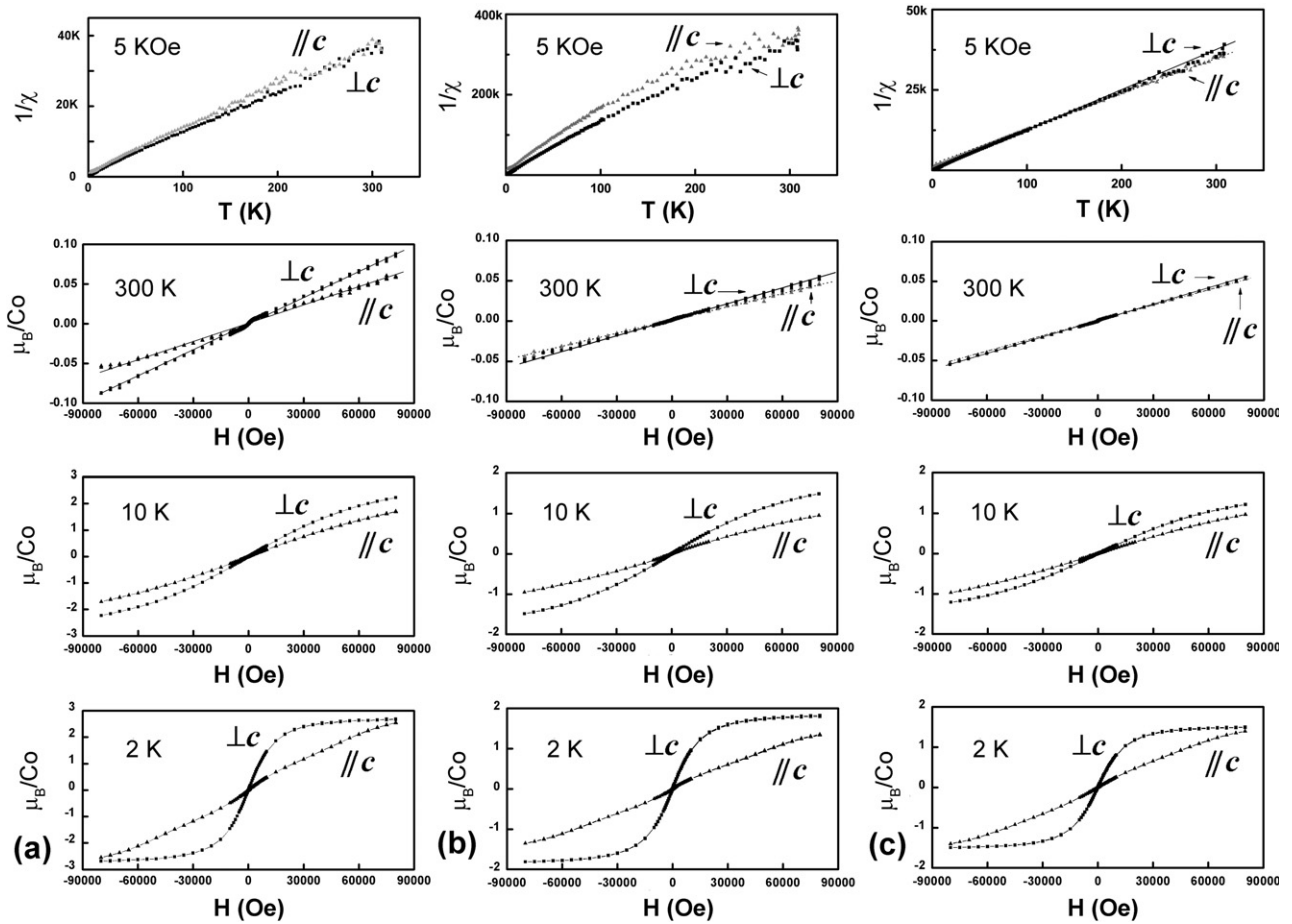


Figure 6. Magnetization curves of as-grown crystals (a) $\text{Zn}_{0.982}\text{Co}_{0.018}\text{O}$, (b) $\text{Zn}_{0.964}\text{Co}_{0.036}\text{O}$, (c) $\text{Zn}_{0.95}\text{Co}_{0.05}\text{O}$ with the magnetic field applied parallel and perpendicular to the c axis of crystal.

directions, the Curie–Weiss temperature Θ obtained from the extrapolation line is approximately 0 K, revealing that all the samples have the typical paramagnetic property from 0 to 300 K.

Conventional superexchange or double-exchange interactions cannot produce long range magnetic order at concentrations of magnetic cations of a few per cent; in order to explain the origin of room temperature ferromagnetism in $\text{Zn}_{1-x}\text{Co}_x\text{O}$ thin film, Coey, Kittilstved *et al* developed a new theory, showing that the ferromagnetic exchange in ZnO DMSs can be mediated by a shallow donor, such as Zn_i [16–18]. The Curie temperature is proportional to the concentrations of magnetic cations and donors. In this work, we found that the $\text{Zn}_{1-x}\text{Co}_x\text{O}$ crystals are all n type and the electronic concentration is about $4\text{--}7.1 \times 10^{18} \text{ cm}^{-3}$ at room temperature, given a magnetic order temperature < 1.65 K. Further treatment of the series of $\text{Zn}_{1-x}\text{Co}_x\text{O}$ crystals with Zn vapor cannot produce a ferromagnetic property either. Thus we conclude that it is hard to achieve a ferromagnetic property for $\text{Zn}_{1-x}\text{Co}_x\text{O}$ crystals with integrated lattices.

The effective moment of Co^{2+} is about $2.7 \mu_B$ in $\text{Zn}_{0.982}\text{Co}_{0.018}\text{O}$ single crystal, which is very close to the saturation moment of Co^{2+} at a tetrahedral site with high spin ($3 \mu_B$). On the basis of the assumption of the ideal crystal lattice with random distribution, 70% of the Co^{2+}

have no first, second or third neighbors and 50% of the Co^{2+} ions have no neighbors closer than the sixth in the $\text{Zn}_{0.982}\text{Co}_{0.018}\text{O}$ crystal [19]. As we know, the Co–O–Co formed antiferromagnetic superexchange interaction in CoO. Thus it is very much possible that most of the Co^{2+} in $\text{Zn}_{0.982}\text{Co}_{0.018}\text{O}$ single crystal can be regarded as isolated magnetic moments, while a small amount of Co^{2+} happens to form Co–O–Co antiferromagnetic couples. With the doping level x increasing, the effective moment of Co^{2+} reduces to $1.82 \mu_B$ for $\text{Zn}_{0.964}\text{Co}_{0.036}\text{O}$ and $1.49 \mu_B$ for $\text{Zn}_{0.95}\text{Co}_{0.05}\text{O}$. The above experimental data reveal that the decreasing tendency of the magnetic moment with the doping level actually is very quick. We further speculate that it is very possible that a greater proportion of Co formed Co–O–Co bound in the crystals when the doping level of Co^{2+} increased. Thus the antiferromagnetic superexchange of these bound Co–O–Co existing in Co^{2+} dilutely doped integrated ZnO samples actually is unfavorable for enhancing the DMS interaction.

Consistently with our previous observation, the series of crystals all show the typical paramagnetic anisotropy property: the magnetic susceptibility in $\perp c$ direction is larger than that in the $\parallel c$ direction [13]. The distinction becomes more apparent when the temperature goes down. Such an easy-plane magnetic anisotropy can be attributed to single-ion anisotropy of DS_z^2 type, which is the origin of the 4A_2 ground state

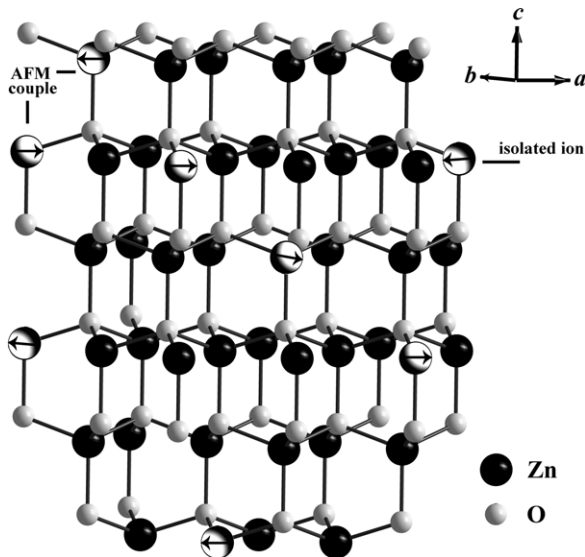


Figure 7. The lattice structure of Co:ZnO. The atoms with arrows indicate Co^{2+} ions which substituted for Zn^{2+} ions.

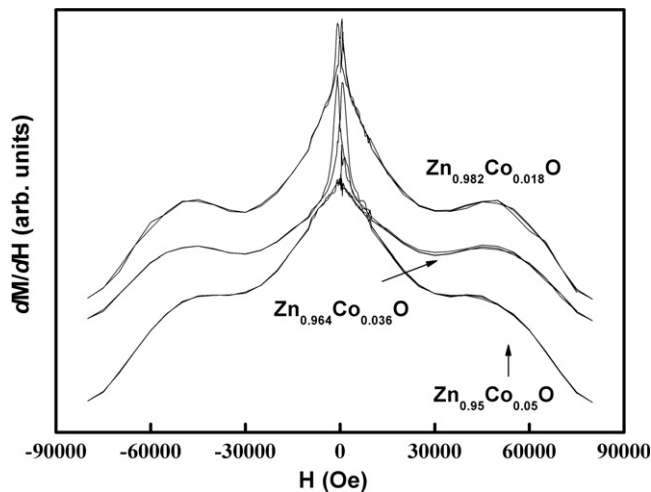


Figure 8. Scheme of magnetization step origin in single-ion anisotropy.

of Co^{2+} in a tetrahedral host lattice [14]. Moreover, the magnetocrystalline anisotropy diminishes when the doping level x increases, consistently with above analysis showing that only a fraction of Co^{2+} can be regarded as ‘isolated Co^{2+} moments’ when the concentration of Co^{2+} increases [19–21]. The distribution of Co^{2+} ions may be like that in figure 7; most of them were isolated while some of them formed Co–O–Co antiferromagnetic couples.

In order to calculate the anisotropy parameter D , dM/dH versus H curves were plotted. As shown in figure 8, magnetization step (MST) peaks were observed at 2 K for the series of crystals. The MST peak (H_c) is fitted as 49.5 ± 0.5 kOe with a Gauss function. By using $2D = g\mu_B H_c$, the Co^{2+} single-ion anisotropy parameter $2D$ for $\text{Zn}_{1-x}\text{Co}_x\text{O}$ single crystals was calculated as 7.5 K, which was in good agreement with the theoretical value [22]. Actually, it was also reported that a MST peak can be found in $\text{Cd}_{1-x}\text{Co}_x\text{S}$

and $\text{Cd}_{1-x}\text{Co}_x\text{Se}$ materials, which was attributed to the single-ion anisotropy of isolated Co^{2+} in the samples [19–21]. Since the single-ion anisotropy parameter D of Co^{2+} in CdSe or CdS lattices was around 1 K, for getting a well-resolved MST, the magnetic experiments had to be carried out at a very low temperature (30 mK), in order to meet the requirement of $k_B T \ll D$. Noticeably, clear magnetization step (MST) peaks can be observed at 2 K for the series of $\text{Zn}_{1-x}\text{Co}_x\text{O}$ crystals. This indicates that the crystal field effect of the ZnO lattice imposed on the Co^{2+} ions is much stronger than those of the CdS and CdSe lattices [19–21].

4. Conclusion

In summary, we have presented a systematic study of the intrinsic magnetism of a series of high quality $\text{Zn}_{1-x}\text{Co}_x\text{O}$ single crystals. It reveals that the origin of the paramagnetic anisotropy of the series of samples is the strong crystal field effect on Co^{2+} ions in the ZnO lattice. The Co^{2+} single-ion anisotropy parameter $2D$ and the effective moment of Co^{2+} in the series of $\text{Zn}_{1-x}\text{Co}_x\text{O}$ single crystals were obtained. The transition of the intrinsic magnetism indicating Co–O–Co antiferromagnetic superexchange in the crystals is unfavorable for enhancing the DMS interaction.

Acknowledgments

Financial support for this study was provided by the Outstanding Youth Fund (50625205), One Hundred Talent Program in the Chinese Academy of Sciences, the National Natural Science Foundation of China (20501021), the Knowledge Innovation Program of the Chinese Academy of Sciences (KJCX2.YW.W01), the Special Project on Science and Technology of Fujian Province (2005HZ1023), Youth Talent of Fujian Province (2006F3140), Fujian Engineering Research Center for Optoelectronic Materials (2007K02, 2005DC105003), the National Key Project of China for Basic Research (2007CB936703). Z Y Wu acknowledges the financial support of the Outstanding Youth Fund (10125523).

References

- [1] Wolf S A, Awschalom D D, Buhrman R A, Daughton J M, von Molnár S, Roukes M L, Chtchelkanova A Y and Treger D M 2001 *Science* **294** 1488
- [2] Ohno H 1998 *Science* **281** 951
- [3] Pearton S J, Norton D P, Ip K, Heo Y W and Steiner T 2005 *Prog. Mater. Sci.* **50** 293
- [4] Dietl T, Ohno H, Matsukura F, Cibert J and Ferrand D 2000 *Science* **287** 1019
- [5] Dietl T, Ohno H and Matsukura F 2001 *Phys. Rev. B* **63** 195205
- [6] Sato K and Katayama-Yoshida H 2000 *Japan. J. Appl. Phys.* **39** 555
- [7] Sato K and Katayama-Yoshida H 2002 *Semicond. Sci. Technol.* **17** 367
- [8] Fukumura T, Jin Z, Ohtomo A, Koinum H and Kawasaki M 1999 *Appl. Phys. Lett.* **75** 3366
- [9] Sharma P, Gupta A, Rao K, Owens F J, Sharma R, Ahuja R, Osorio-Guillen J, Johansson B and Gehring G 2003 *Nat. Mater.* **2** 673

- [10] Park J H, Kim M G, Jang H M, Ryu S and Kim Y M 2004 *Appl. Phys. Lett.* **84** 1338
- [11] Prellier W, Fouchet A, Mercey B, Simon C and Raveau B 2003 *Appl. Phys. Lett.* **82** 3490
- [12] Risbud A S, Spaldin N A, Chen Z Q, Stemmer S and Seshadri R 2003 *Phys. Rev. B* **68** 205202
- [13] Li W, Kang Q Q, Lin Z, Chu W S, Chen D L, Wu Z Y, Yan Y, Chen D G and Huang F 2006 *Appl. Phys. Lett.* **89** 112507
- [14] Sati P *et al* 2006 *Phys. Rev. Lett.* **96** 017203
- [15] Kim J H, Kim H, Kim D, Yoon S G and Choo W K 2004 *Solid State Commun.* **131** 677
- [16] Coey J M D, Venkatesan M and Fitzgerald C B 2005 *Nat. Mater.* **4** 173
- [17] Kittilstved K R, Schwartz D A, Tuan A C, Heald S M, Chambers S A and Gamelin D R 2006 *Phys. Rev. Lett.* **97** 037203
- [18] Kittilstved K R, Liu W K and Gamelin D R 2006 *Nat. Mater.* **5** 291
- [19] Bindilatti V, Oliveira N F, Shapira Y Jr, Vu T Q, Heiman D and Demianiuk M 1993 *Solid State Commun.* **87** 759
- [20] Shapira Y and Bindilatti V 2002 *J. Appl. Phys.* **92** 4155
- [21] Isber S, Averous M, Shapira Y, Bindilatti V, Anisimov A N, Oliveira N F, Orera V M and Demianiuk M 1995 *Phys. Rev. B* **51** 15211
- [22] Kuzian R O, Daré A M, Sati P and Hayn R 2006 *Phys. Rev. B* **74** 155201